Available online at www.sciencedirect.com
SCIENCE DIRECT
Polymer 47 (2006) 5810–5820
polymer
www.elsevier.com/locate/polymer

Molecular dynamics and crystallization kinetics in PSMA14/PCL blends

Vittoria Balsamo [a,*], Dinorah Newman [b], Laura Gouveia [a], Lenín Herrera [a], Mario Grimau [a], Estrella Laredo [b,*]

[a] *Materials Science Department, Universidad Simón Bolívar, Apartado 89000, Caracas 1080-A, Venezuela*
[b] *Physics Department, Universidad Simón Bolívar, Apartado 89000, Caracas 1080-A, Venezuela*

Received 3 May 2006; received in revised form 8 June 2006; accepted 12 June 2006
Available online 30 June 2006

Abstract

The effect of blending poly(styrene-*co*-maleic anhydride) with 14 mol% MA (PSMA14) with poly(ε-caprolactone) (PCL) is studied by calorimetry, X-ray diffraction, dielectric techniques, and microscopy. Variations in PCL crystallization, melting temperatures and crystallinity degree were observed. Additionally, the presence of a wide and asymmetric enthalpic step, whose position follows Fox predictions, demonstrates miscibility between the blend components. This is in agreement with the interlamellar location of PSMA14. Thermally stimulated depolarization techniques evidenced two segmental dynamics, with distinct compositional variations due to the local differences in composition perceived by each component as a consequence of chain connectivity. The two effective glass transition temperatures vary with composition, in agreement with the self-concentration model predictions when using the Kuhn's segment length for each component. From isothermal crystallizations a marked depression of the PCL equilibrium melting point $\left(T_m^o\right)$ is observed in the blends together with an increase in the half-crystallization times, $\tau^{1/2}$, as the content of PSMA14 grows. PCL-rich blends exhibited ring-banded spherulites, with a ring periodicity that increased with crystallization temperature and with PSMA14 content. Preliminary results of the phase separation process are given from samples that were thermally treated under different conditions.

Keywords: Blends; Self-concentration model; Crystallization in blends

1. Introduction

Semicrystalline polymers are very interesting materials; they range from commodity plastics to high-performance engineering resins. In fact, roughly half to two-thirds of the most used polymers are semicrystalline or crystallizable [1]. A growing number of commercial materials are miscible blends of two or more polymers in which at least one of the components is a crystallizable one. However, the crystalline microstructure, crystallization kinetics and phase structure are not well understood as in neat semicrystalline materials. On the other hand, with the increased use of sensitive techniques capable of probing blend miscibility at very small scales, dynamic heterogeneities have been evidenced in many miscible systems whose components were amorphous in most of the previous studies [2–4].

One semicrystalline polymer that has been widely used as a blend component is the poly(ε-caprolactone) (PCL), a biodegradable aliphatic polyester that exhibits miscibility with a variety of polymers including poly(vinyl chloride) (PVC) [5–8], chlorinated polyethylene (CPE) [9], poly(hydroxy ether of bisphenol A) [10], poly(4-vinylphenol) [11], polycarbonate of bisphenol A (PC) [4,12,13], and polystyrene oligomers [14] among others.

Blends of PCL with high molecular weight polystyrene have proven to be immiscible, but the introduction of functional groups through chemical modification or copolymerization

* Corresponding authors. Tel.: +58 212 9063388; fax: +58 212 9063536.
E-mail addresses: vbalsamo@usb.ve (V. Balsamo), elaredo@usb.ve (E. Laredo).

0032-3861/$ - see front matter © 2006 Elsevier Ltd. All rights reserved.
doi:10.1016/j.polymer.2006.06.019

has shown to be an effective route to induce miscibility with PCL. For example, PCL is miscible with poly(styrene-*co*-acrylonitrile) (SAN) with an acrylonitrile content in the SAN copolymer that varies from 8 to 28 wt% [15–18]. Another possibility is the mixing of PCL with poly(styrene-*co*-maleic anhydride) (PSMA). Defiew et al. [19] reported miscibility for PCL blended with PSMA copolymers with 14 or 25 wt% maleic anhydride, which exhibit only one glass transition, T_g, at intermediate temperatures. PSMA is found to segregate interlamellarly during the crystallization process of PCL over the whole composition and temperature range. Later, Vanneste and Groeninckx [20] studied the ternary blend PCL/SAN15/SMA14 and showed a dependency of the miscibility on the molecular weight of the components. It should be emphasized that in these works the blends were prepared from cast solutions, and that they attributed the observed behavior to physical interactions among the components. Balsamo et al. [21] demonstrated through spectroscopic methods that, even if the blends are prepared by melt-extrusion, neither chemical reactions among the polymers nor degradation takes place. In the same work, preliminary results on the thermal and morphological behaviors were presented.

In a miscible blend, in addition to the intermediate and broad glass transition, with an asymmetric character observed in the calorimetric scans, two cooperative dynamics have been recorded, both at intermediate temperatures between the homopolymers' T_gs. This ''dynamic heterogeneity'' has been widely studied by dielectric spectroscopy [2] and thermally stimulated depolarization currents, TSDC [4,13] when the blend components are polar. One approach to account for the existence of two segmental dynamics is the existence of local concentration variations resulting from the effect of thermal concentration fluctuations [22]. Another approach by Lodge and McLeish [23] emphasizes chain connectivity effects, which result in one effective glass transition for each component, $T_{gA}^{eff}(\phi)$and $T_{gB}^{eff}(\phi)$, based on the average local composition calculated from the ''self-concentration'' perceived by each of them. These effective compositions differ from the bulk one depending on the relevant length scale for the cooperative mobility, which is taken as the Kuhn's length of each homopolymer. The $T_g^{eff}(\phi)$'s compositional variations for each component are also predicted by the dynamic heterogeneities explained by the self-concentration model, if the variation of the bulk T_g with composition is known.

The aim of this work is to investigate in detail in the homogeneous blend system PSMA14/PCL, the effect of blending on the different mobility scales detected by TSDC experiments over a wide temperature and concentration range, and the consequences that such blending has on the crystallization of the PCL. Wide Angle X-Ray Scattering (WAXS), Transmission Electron Microscopy (TEM) and Polarizing Optical Microscopy will complement the quantitative information presented here on the morphology of these miscible blends. Several calorimetric and morphological results about the phase separation process that occurs at high temperatures are also given.

2. Experimental

2.1. Materials

We used a poly(ε-caprolactone) (PCL) Tone-787, manufactured by Union Carbide ($\overline{M}_n$ = 73 kg/mol, $\overline{M}_w$ = 112 kg/mol), and a poly(styrene-*co*-maleic anhydride) (PSMA14) copolymer with 14 mol% of maleic anhydride (MA) units, where MA units are randomly distributed, purchased from Aldrich Chemical Co, Inc. ($\overline{M}_n$ = 100 kg/mol, $\overline{M}_w$ = 174 kg/mol). Blends of different compositions (PSMA14/PCL: 0/100, 10/90, 30/70, 40/60, 70/30, 90/10, 100/0) were prepared by melt-mixing in a laboratory scale screw extruder at temperatures that were set at 180–235 °C in the die and in the barrel zone, depending on blend composition. Each blend was processed twice to ensure their homogeneity.

From the melt-mixed blends compression-molded sheets were prepared. The molding was performed between Kapton© sheets at 170–195 °C, depending on composition. Then, the films were quenched in cold water.

2.2. Differential Scanning Calorimetry

For the Differential Scanning Calorimetry (DSC) studies, a Perkin–Elmer DSC-7 Calorimeter was used. Small disc-shaped samples were cut (13.0 ± 0.1 mg) from the compression-molded sheets and encapsulated in aluminum pans. High purity dry nitrogen was used as inert atmosphere. For measurements under −20 °C a Perkin–Elmer PYRIS-1 calorimeter was used. The general calorimetric behavior was studied by heating and cooling the samples at a rate of 10 °C/min after they were held in the melt at 170 °C for 5 min to erase the previous thermal history. Isothermal crystallizations were performed after the samples were heated to 170 °C and annealed at that temperature for 5 min. Then, they were quenched at a rate of 80 °C/min to a selected crystallization temperature, T_c, where they were held for a crystallization time, t_c, equal to three times the crystallization time deduced from the isothermal exothermic peak. Finally, a heating scan from T_c to 170 °C was recorded at 10 °C/min.

2.3. WAXS experiments

The films for all blend compositions were studied by X-ray diffraction at wide angles. The WAXS experiments were performed in a Philips Automatic diffractometer by using Cu Kα, Ni-filtered radiation. The spectra are recorded in an angular range $5° < 2\theta < 40°$ at room temperature. The interplanar spacings that can be measured correspond to the main reflections originated by crystalline PCL that are superimposed to the amorphous halos of both PCL and PSMA14. PCL crystallizes in the space group $P2_12_12_1$ with a = 7.496 Å, b = 4.974 Å, c = 17.297 Å, and gives main reflections at 2θ values of 15.64° (102), 21.40° (110), 22.05° (111), 23.70° (200), 24.3° (201), and 29.85° (210) [24]. The crystallinity degree, X_c, of the PCL in each blend was determined by a peak decomposition of the WAXS blend trace

which includes the crystalline sharp peaks and the wide halos identified in the amorphous homopolymers spectra. These degrees of crystallinity are very useful in the interpretation of the TSDC spectra as they reflect the state of the material at room temperature. The amount of mobile amorphous phase which is observed by TSDC should be nearly the same as that given by $(1 - X_c)$ if no constrains to its mobility exist.

2.4. Transmission Electron Microscopy

Pyramidal samples of the compression-molded sheets were introduced in a 2% w/v RuO_4 solution for three weeks. Ultrathin sections (~40 nm) from the stained samples were cut at −100 °C using a Reicher-Jung FC4 Ultramicrotome equipped with a diamond knife. Electron micrographs were taken with a Jeol Jem-1220 microscope, operating at 120 kV in the bright field mode.

2.5. Optical Microscopy

A Zeiss polarizing optical microscope coupled with a hot-stage was used to investigate the superstructure formation in isothermally crystallized samples that were previously cut in a microtome. These sections were held in the melt for 5 min and quenched down to the chosen crystallization temperature, T_c under polarized light.

2.6. Thermally stimulated depolarization currents

TSDC experiments were performed in a cell and measuring system designed in our laboratory [25]. During the polarization step an external electric field, E_p (typically 1 MV/m), is applied to the sample at temperatures, T_p, sufficiently high to orient the dipolar species under study. During this step the measuring cell is filled with pure N_2 gas, at a pressure of 600 mTorr. The built-in polarization is frozen-in by a rapid quenching to liquid nitrogen temperature. The cell is evacuated and filled with pure He gas which is the interchange gas, and the return to the random orientation state of the previously oriented dipoles is thermally stimulated by a temperature increase at a linear rate, $b_h = 0.07\ K\ s^{-1}$, the depolarization current being recorded by a Keathley 642 electrometer. The disc-shaped sample, 20 mm in diameter and around 300 μm thick, is located in the TSDC cryostat between two vertical metallic discs lightly spring-loaded. The sensitivity of our system is 10^{-16} A, and the data acquisition is fully automatic. One of the advantages of the TSDC technique is its capability to isolate a particular relaxation from its neighboring peaks by carefully choosing the polarization conditions. The presence of peaks located at higher temperature than the mode under study is minimized by polarizing the sample near the maximum of that peak. At this temperature the relaxation time of the species, whose contribution has to be eliminated, is long and the dipoles responsible for this polarization are not able to reorient in significant amount during the polarization time. Also, by partially discharging (peak cleaning) the low temperature side of a TSDC complex peak, the contribution of modes whose relaxation occurs at lower temperatures is minimized.

3. Results and discussion

3.1. Standard calorimetric behavior and morphology

In a previous work the thermal stability of PSMA14/PCL blends under different conditions was tested [21]. By using FTIR and ^1H NMR it was found that no significant chemical reactions take place between the components, even after maintaining the samples at 210 °C for 180 min. Thus, all changes exhibited by the blends are the result of physical interactions among the homopolymers (PSMA14 and PCL).

Fig. 1 shows DSC cooling and heating scans of the PSMA14/PCL blends investigated in this study. One advantage of this blend system is the wide difference among the glass transition temperatures of the homopolymers, $T_{gPCL} = -63.4$ °C, $T_{gPSMA} = 127.1$ °C as measured by DSC. The semicrystalline PCL crystallizes and melts at 30.6 °C and 56.7 °C, respectively. Upon cooling, only those blends with PCL contents higher than 60 wt% exhibit crystallization, and the exotherm is shifted to lower temperatures as the PSMA14 content increases. Blends that do not crystallize exhibit a wide single calorimetric step at T_g, which is shifted to lower temperatures, compared to neat PSMA14. Upon heating, a depression of the PCL melting point, T_m, is observed. In Fig. 1b one can see that with increasing PSMA14 content, the crystallization of the PCL fraction is hindered, and for 60 wt% PCL, part of the crystallization takes place on heating (cold crystallization). However, even after such crystallization, the normalized heat of fusion is less than that of neat PCL. The depression of the PCL crystallization and melting temperatures, the impeded crystallization of the PCL when its content is lower than 60%, as well as the observation of one T_g located in between those of the homopolymers are indicative of the components' miscibility. The shift of the thermal transitions results from the addition of a miscible component that is more rigid; therefore, the molecular transport of the crystallizable segments towards the crystalline front is perturbed, and higher supercoolings are needed to be crystallized. For PSMA14 contents higher than 30 wt%, the blend glass transition is located at temperatures above the PCL's T_c. This is the reason for the absence of crystalline regions in these blends. Similar results have been reported for blends of PCL with SAN, PVC or Phenoxi [5,9,10,16,18,26–28].

Fig. 2 shows WAXS traces recorded for the homopolymers and PSMA14/PCL blends of various compositions. The Bragg reflections from the PCL crystalline regions are clearly visible for PCL contents greater or equal to 30% in weight. The PCL crystallinity degree was determined by decomposing the signal into the broad amorphous halos originated from the PCL and PSMA amorphous regions and the Bragg peaks caused by the PCL crystalline lamellae. Its variation is plotted in the inset of Fig. 2 as a function of the nominal composition of the blend amorphous phase. The crystallinity degrees measured by WAXS at room temperature are in very good agreement

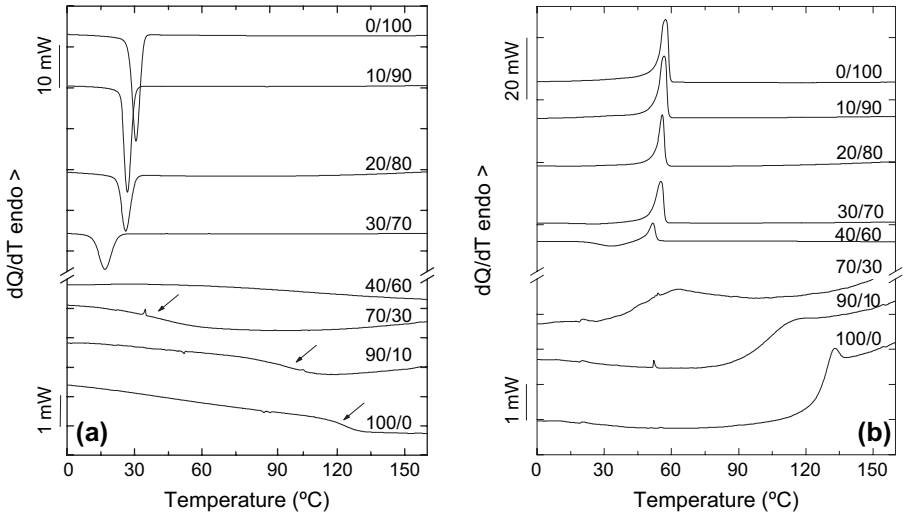

Fig. 1. DSC (a) cooling and (b) heating scans (10 °C/min) of the PSMA14/PCL blends. The compositions are indicated on each trace. The arrows show the glass transition.

with those determined from the first heating DSC scans (not shown here).

In order to investigate how the morphology of the blends can be affected in comparison to neat PCL, a study of the lamellar morphology was performed in PSMA14/PCL 30/70 using Transmission Electron Microscopy (TEM). Fig. 3a shows the TEM micrograph of pure PCL, stained with RuO_4. A lamellar morphology is clearly identified, in which the bright zones correspond to the crystalline lamellae, and the dark ones to the stained amorphous interlamellar regions. A homogeneous distribution of long lamellae can be observed. The 30/70 blend (Fig. 3b) also shows a lamellar morphology, but unlike neat PCL, the lamellae are shorter, thinner, and some of them are branched. The absence of segregated dark regions indicates, in agreement with the calorimetric results that the PSMA14 is located in the interlamellar regions. No interfibrillar location of the PSMA14 is observed. Interfibrillar segregation is understood whenever the amorphous component is

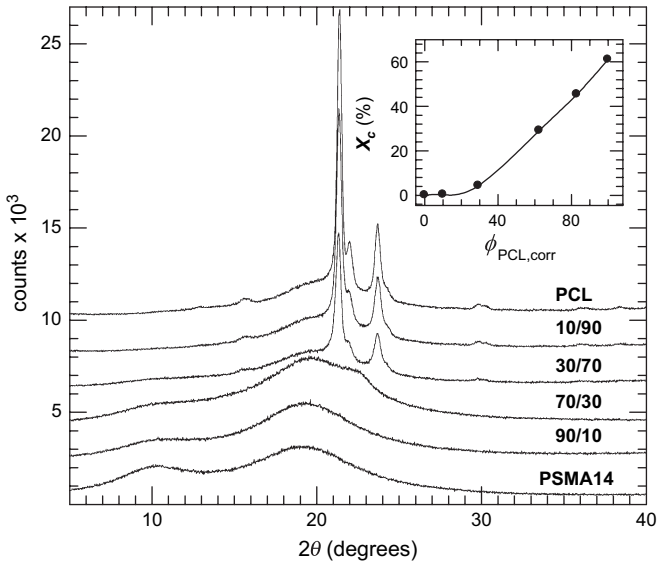

Fig. 2. WAXS spectra (Cu Kα, Ni-filtered radiation) of the PSMA14/PCL blends, the global blend composition is indicated on each trace. The inset represents the variation of the PCL degree of crystallinity as a function of the amorphous content of the PCL phase.

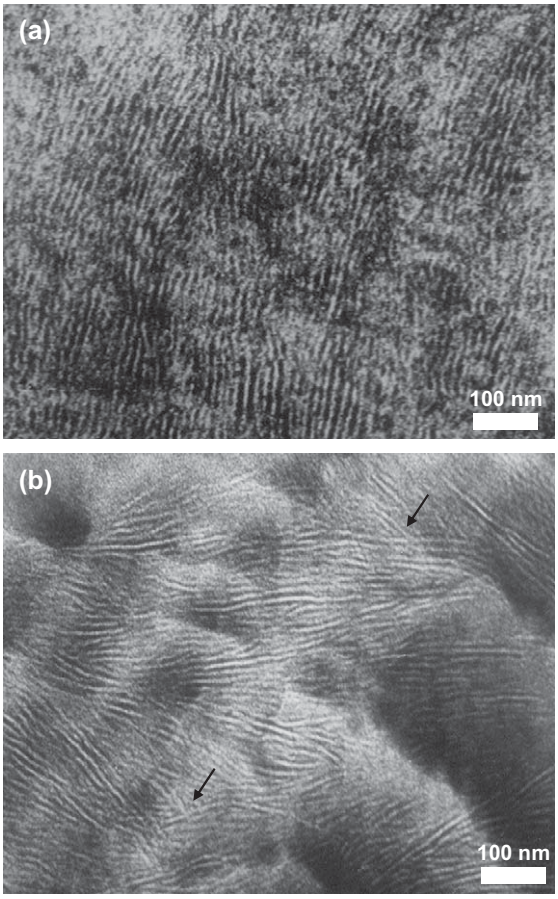

Fig. 3. TEM micrographs of (a) PCL and (b) PSMA14/PCL 30/70, stained with RuO_4.

located between groups of lamellae in such a way that the segregated domains exceed the interlamellar spacings [5,9,10,28]. On the other hand, it should be noted that the darker zones observed in Fig. 3b should not be assigned to such segregated domains; they correspond to TEM artifacts produced by the non-uniform cutting of the sections or to undulations present in it.

This morphology agrees with findings of Defiew et al., who observed an increase of the long period by means of SAXS with the addition of PSMA [19]. This type of behavior has also been found in SAN/PCL blends. Although it is known that the estimation of lamellar thicknesses from TEM micrographs usually gives underestimated values, an average lamellar thickness was determined for both neat PCL and PCL in the 70/30 blend for comparison purposes only. Thus, we obtained values of 61 ± 7 Å and 47 ± 8 Å, respectively. The reduction of the PCL lamellar thickness in the blend is another evidence of the miscibility between PSMA14 and PCL. Such depression of the lamellar thickness is related to the PCL melting-point depression determined from DSC heating scans, especially if it is noted that the PCL component in the blend crystallizes at a lower temperature.

In a homogenous polymer blend, the crystallization of one of the components leads to a variety of superstructures that depend on the lamellar array. The most common form is the ''spherulitic'' one, but even in this case some variations can be found. Fig. 4 shows the spherulites formed after isothermal crystallization at the indicated temperatures. It is observed that in addition to the typical Maltese Cross, extinction rings appear, originating the so called ring-banded spherulites. This kind of superstructures has been observed, for example, in blends of PCL with SAN [18,29,30] and PVC [5] as well as in block copolymers [31–33]. In the images it can be also appreciated that the spherulites fill all the space; this indicates the absence of interspherulitic segregation. In all cases, a linear increase of the radii of the spherulites with time was found until their impingement, evidencing that the growth rate is not controlled by diffusion. These results are in agreement with the interlamellar location of the PSMA14 evidenced here with TEM, and are the consequence of the low flexibility of the PSMA chains and its affinity towards the PCL.

It is well known that banding is the result of the cooperative twisting of the lamellae during growth. Although such twisting has been associated with internal stresses produced on the lamellae surfaces, the reason for its occurrence is still controversial [34]. In the case of polymer blends, it has been additionally reported that the periodicity, ρ_s, of the rings depends on composition [35]. In order to characterize the superstructure, the periodicity of the rings was measured in PSMA14/PCL 20/80 and 30/70. The results are presented in Fig. 5, where it can be observed that the periodicity increases with the content of the amorphous component, a fact that is contrary to the results obtained by other authors [33,36,37] in blends containing PCL. Nevertheless, Briber and Khoury reported a similar trend in poly(vinylene fluoride)/poly(ethyl acrylate) blends [38,39]. This could be related to the dependence of the interaction parameter on composition; this aspect is yet under study. Additionally, the periodicity markedly increases with the crystallization temperature, due to the higher segmental mobility within the blend.

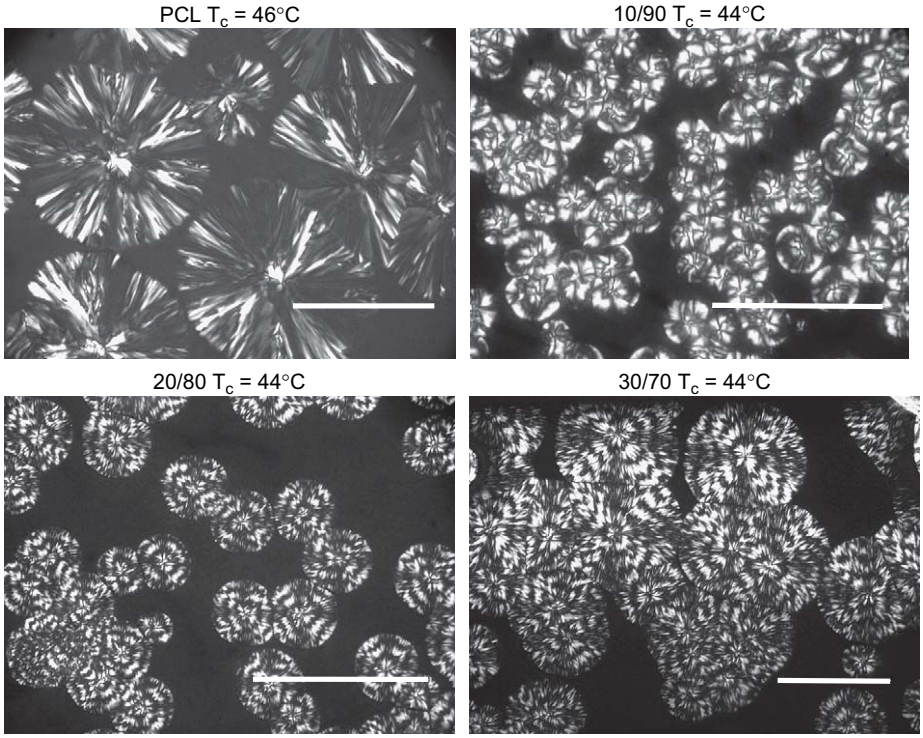

Fig. 4. POM images obtained during isothermal crystallization of PSMA14/PCL blends at the indicated crystallization temperatures. The bars represent 100 μm.

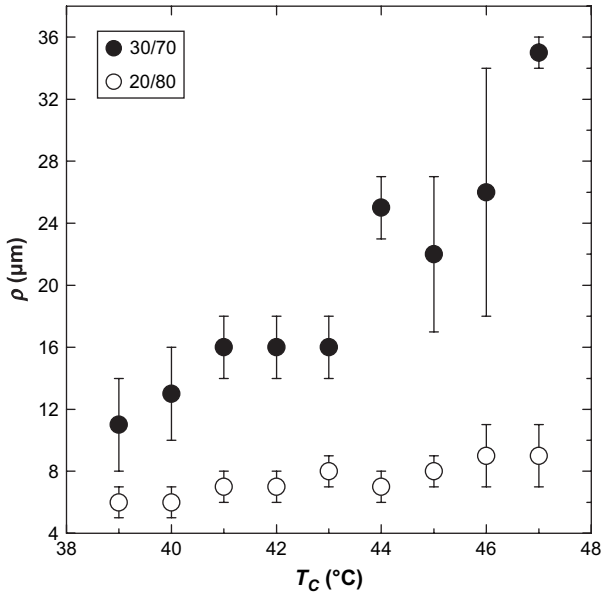

Fig. 5. Dependence of the ring periodicity measured from POM micrographs as a function of crystallization temperature for PSMA14/PCL 30/70 and 20/80.

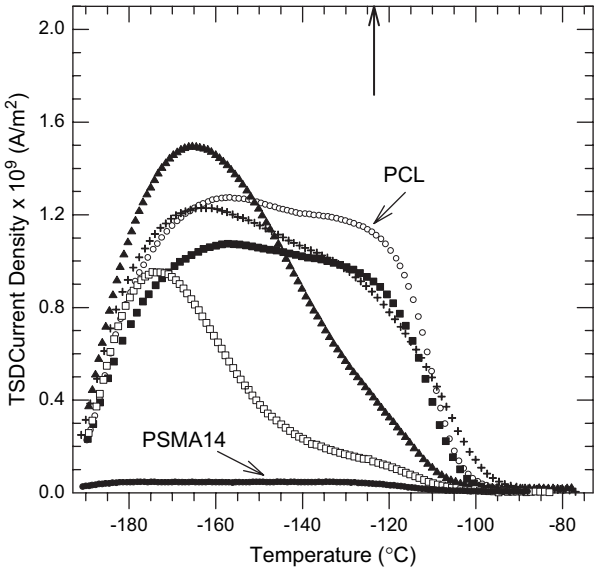

Fig. 6. Low-temperature TSDC spectra of the PSMA14/PCL blends with bulk compositions: (○) 0/100; (■) 10/90; (✚) 30/70; (▲) 70/30; (□) 90/10; (●) 100/0. The polarization temperature is indicated by the vertical arrow.

3.2. TSDC results

Dielectric techniques are used to follow the mobility at different scales in polymeric systems. At low temperatures, weak signals are recorded which correspond to the secondary relaxations usually labelled γ and β with increasing temperatures. These localized motions of the chain are of restricted and increasing amplitude on going from the γ to the β mode, and their Arrhenius activation energies are low enough to allow their detection in the low-temperature range. It is to be noted that the equivalent frequency of our TSDC experiments with a heating rate of 0.07 °C/s is around 30 mHz, and due to the high sensitivity of our measuring system these relaxations are precisely detected. In the temperature range where the secondary relaxations take place no changes in crystallinity are expected; in this way, the area under the curves, which is representative of the number of orientable dipoles, is indicative of the amount of mobile amorphous phase at room temperature.

The low-temperature TSDC spectra of the homopolymers and blends are represented in Fig. 6 for the same polarization conditions ($T_p = -123$ °C) and sample size. The contribution of the PSMA14 to the blend polarization for the secondary relaxation modes is very small and the changes in area and profile are mainly due to the localized motions of the PCL chains in the amorphous regions of the blends. In Fig. 7, the polarization calculated from the area under the low-temperature relaxations is plotted against the polarization calculated from the weighted contributions of the amorphous content of each component. Blends richer in PSMA14, where the crystallinity is negligible up to the 70/30 composition, follow the expected variation. On the contrary, blends with the higher PCL crystallinity; i.e. 30/70 and 10/90, present a polarization which is significantly lower than expected; this result shows that in the presence of PCL crystalline lamellae in considerable proportions, in addition to PSMA14, the PCL local molecular mobility is restricted.

The PCL secondary relaxations have been thoroughly studied in the PCL homopolymer by dielectric spectroscopy [40], and the main results are as follows: (a) the γ mode is more intense in dry samples and as the moisture content increases the β mode predominates; (b) their position and profile are not sensitive to the molecular weight; (c) a merging of the α and β modes at high temperatures and low frequencies, and a second merging at still higher temperatures of the α β and γ modes is observed. Upon blending PCL with polycarbonate, PC, it has been shown that blending surely affects the local scale mobility, since the number of mobile dipoles is higher than expected at high PCL concentrations in spite of the existence of PCL high crystallinity [4]. The observed

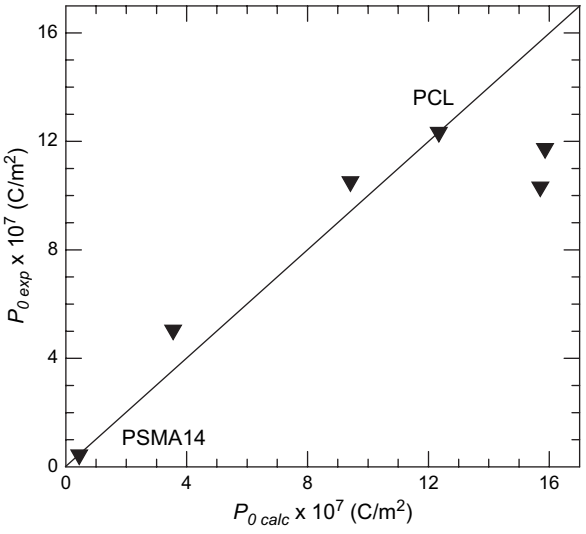

Fig. 7. Variation of the polarization experimentally detected vs. the weighted contribution of both blend components.

variations of the polarization induced by short-range motions of the two polar components in the PC/PCL system were explained by assuming the existence of a PC rigid amorphous fraction which is rendered mobile by the addition of increasing amounts of PCL. In the present study, where the polarity of PSMA14 is almost negligible, the variation of the low-temperature PCL polarization in the blends is opposite. As the PCL concentration increases, the observed reduction in the number of mobile dipoles originating from the secondary relaxations might be attributed to constrains imposed by the combination of the presence of rigid PSMA14 chains and the PCL crystalline lamellae. These effects on the chain mobility at a local scale confirm the excellent miscibility encountered in the PSMA14/PCL system.

Another important change in the short-range mobility promoted by the addition of PSMA14 to PCL is the variation observed in the profile of the low-temperature spectra as seen in Fig. 6. At low PSMA14 concentrations the PCL γ and β relaxations have relative contributions that are comparable to those observed in pure PCL. As the PSMA14 concentration exceeds 30%, there is a significant relative decrease in the contribution of the β mode as compared to the γ relaxation. The γ mode, being located at lower temperature, has been associated to shorter range mobility than that at the origin of the β mode [4,25]. The reduction in the intensity of the β mode is caused by the restrictions imposed by the PSMA14 on molecular motions whose complexity is higher, and they require a larger volume than necessary for the almost isolated dipolar reorientations associated to the γ mode.

The dielectric spectrum of polar homopolymers presents at higher temperatures the primary relaxation, α mode, which is the dielectric manifestation of the glass transition temperature and is representative of the cooperative mobility of the molecular chains. In Fig. 8 the well defined α peaks of the homopolymers are located at $T_{M\alpha PCL} = -(67.5 \pm 0.5)$ °C, $T_{M\alpha PSMA14} = (124.8 \pm 0.5)$ °C, in good agreement with the

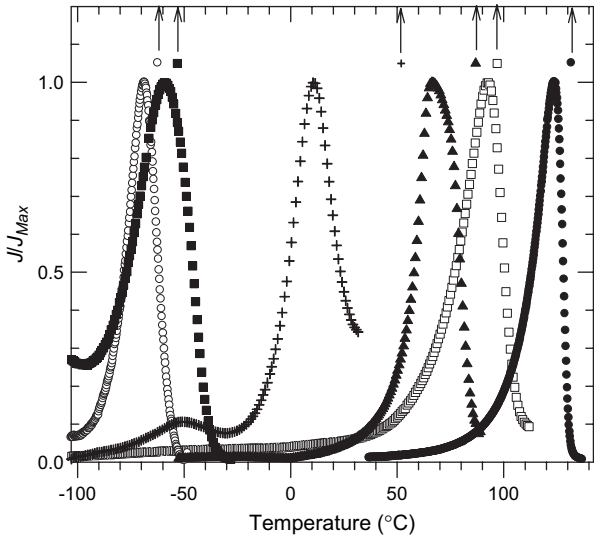

Fig. 8. Segmental modes in PSMA14/PCL blends with nominal compositions: (○) 0/100; (■) 10/90; (✚) 30/70; (▲) 70/30; (□) 90/10; (●) 100/0. The polarization temperature for each blend is indicated by vertical arrows.

T_gs determined by DSC. The normalized depolarization currents, J/J_{Max}, are plotted as a function of temperature for all the blend compositions studied here. In this miscible system, where the DSC traces drawn in Fig. 1 show a single and asymmetrically broadened calorimetric step, the more sensitive TSDC probe allows to distinguish two cooperative modes located at intermediate temperatures between the homopolymers' T_gs in agreement with the predictions of the self-concentration model [23]. These two modes are clearly visible in Fig. 8 for the 30/70 TSDC trace, i.e. $T_{gA}^{eff} = -49$ °C and $T_{gB}^{eff} = 11$ °C. When the PCL is the minor blend component the detection of the low-temperature component needs the very careful choice of polarization and detection conditions as the intensity of the broad low T_g curve is very weak. For example to be able to determine T_{gA}^{eff} for the 70/30 blend the polarization temperature was 87 °C which is above the two T_gs, and the low-temperature tail of the intense peak was amplified by a factor of 20. In this way we determined $T_{gA}^{eff} = (-18 \pm 1)$ °C and $T_{gB}^{eff} = +(66.5 \pm 0.5)$ °C. Also, for the 10/90 nominal composition the high temperature effective T_g is not observed as there exists in the same temperature range an intense interfacial peak. It is to be noted that the experimental evidence of two T_gs is rather scarce in the literature as most works have been performed on blends with only one polar component. Previous works with TSDC technique, which seems the most appropriate to evidence the existence of two T_gs are on PC/PCL [4] and PVME/P*o*ClS [41]. In the first one the two T_gs are more easily visualized than in the present work as the polarization built up in PC is much higher than in the PSMA component.

The existence of two T_gs is associated to the high and low effective glass transition temperatures, T_{gA}^{eff} and T_{gB}^{eff} that are predicted by the Lodge and McLeish model [23] for miscible B/A blends. They are attributed to the concentration fluctuations in the cooperative rearranging regions of each component, PCL and PSMA14, respectively. These effective glass transition temperatures can be evaluated by calculating the self-concentration which is the average local composition perceived by each blend component; these local compositions might be quite different from that of the bulk as the flexibility of the polymer chain decreases. For the calculation of the self-concentration for PCL, the Kuhn's segment length was used, $l_{KPCL} = 7.0$ Å. The self-concentration is given by

$$\phi_s = \frac{C_\infty M_0}{k \rho N_0 l_K^3} \tag{1}$$

where M_0 is the repeat unit molar mass, k is the number of main chain bonds per repeat unit, ρ is the polymer density and N_0 is the Avogadro number. The resulting PCL self-concentration is $\phi_{sA} = 0.33$. For the PSMA component the self-concentration was taken equal to 0.27, following the parameters for PS of Fetters et al. [42].

The bulk T_g compositional variation calculated with Fox equation (continuous line) is compared to the DSC T_gs (empty circles), in Fig. 9. An excellent agreement was found in the case of the PSMA14/PCL system when amorphous phase

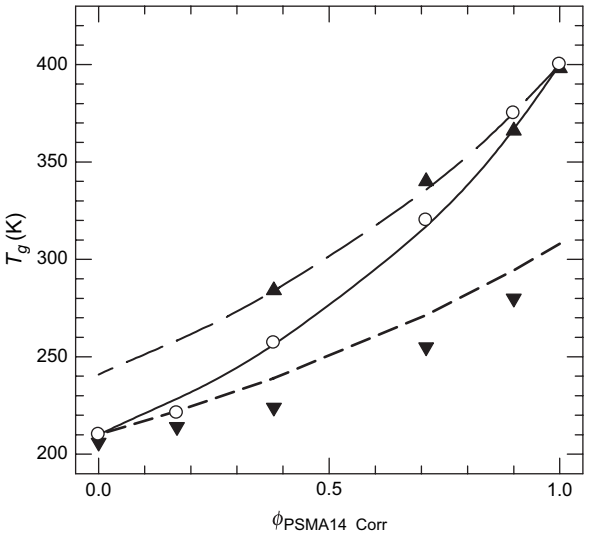

Fig. 9. Variation of glass transition temperatures of PSMA14/PCL blends: (○) DSC results; (—) Bulk T_gs calculated with Fox equation; (▲) TSDC values for T_{gB}^{eff}; (— — —) T_{gB}^{eff} predicted by the self-concentration model; (▼) TSDC values for T_{gA}^{eff}; (▬▬) T_{gA}^{eff} predicted by the self-concentration model.

compositions are corrected from crystallinity. Following Lodge and McLeish [23] this behavior is assumed to be valid for the composition variation of the two effective T_gs when using the effective concentrations instead of the nominal ones. Then, T_{gA}^{eff} and T_{gB}^{eff} were calculated by using the Fox equation

$$T_{gA}^{eff} = \left(\frac{\phi_{effA}}{T_{gA}} + \frac{1-\phi_{effA}}{T_{gB}}\right)^{-1} \quad (2)$$

with the effective concentrations, ϕ_{eff}, being given for each component A and B by:

$$\phi_{eff} = \phi_s + (1-\phi_s)\phi \quad (3)$$

where ϕ is the corrected amorphous blend composition. The results plotted in Fig. 9 show the good agreement found among the TSDC high and low effective T_gs, and the predictions of the self-concentration model by using the Kuhn's length for each component of the PSMA14/PCL blends. It is to be noted that the use of a polystyrene copolymerized with 14% of maleic anhydride does not seem to affect the chain characteristics as the high T_g variation with blend composition is very well described by the model when the PS self-concentration is used.

The PSMA14/PCL mixtures are another example of miscible blends with concentration fluctuations where only one of the components is crystallizable. In the case of the PC/PCL blends previously studied [4,13], where the two components were crystallizable, the PC crystallization lead to a phase separation in the amorphous state as was demonstrated by TSDC and isothermal crystallization studies. In order to study the effect of the miscibility encountered in PSMA14/PCL blends on the PCL crystallization process, isothermal crystallization experiments were performed and the results are described below.

3.3. Isothermal behavior and effect of the temperature

DSC and TSDC results have proved the existence of dynamic heterogeneities in the miscible PSMA/PCL blends. The effect of isothermal crystallization of PCL in the blends was carried out for the PSMA14/PCL 30/70 and 10/90 compositions. Fig. 10 shows DSC heating scans obtained after isothermal crystallizations at different temperatures. The figure reveals the presence of two endotherms in PSMA14/PCL 30/70 and 10/90, a weak one located at low temperature (indicated by arrows in Fig. 10b, and that was not observed in the pure PCL) and a more intense one at higher temperatures; both shifted to higher temperatures as T_c increases, the low melting endotherm being more evident as the PSMA14 content increases, in agreement with previous works [19,20]. The appearance of multiple endotherms in polymers has been reported in many other systems, and different explanations have been given for their origin;

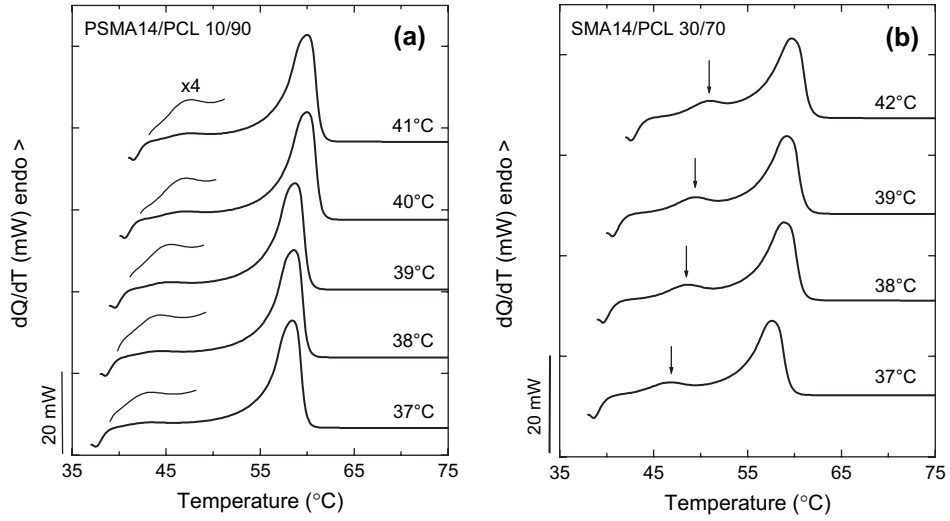

Fig. 10. DSC heating scans (10 °C/min) of PSMA14/PCL (a) 10/90 and (b) 30/70 after isothermal crystallization at the indicated temperatures.

secondary crystallization and partial melting–recrystallization are the most common. The characteristics of the peaks indicate that the low melting endotherm is due to a secondary crystallization process in the blends. An evidence of this is that the lower melting peak appears in the advanced stages of the isothermal crystallization; i.e. at higher crystallization times. In addition, experiments performed at different heating rates (not shown here) excluded the possibility of a partial melting-recrystallization process. In a miscible blend the crystallization of a polymer involves the diffusion of the crystallizable component towards the crystalline front and segregation of the amorphous component farther away from the nucleus. Under these conditions, if the amorphous component has a T_g that is higher than that of the crystallizable component, there is not enough time for the insertion of all PCL chains in the spherulite growth process. Thus, once the spherulites have been formed, the rest of PCL crystallizes with the formation of thinner lamellae that melt at lower temperature.

Melting-point depression has been extensively used to evaluate the miscibility in polymer blends. The usual approach to determine T_m^o is the Hoffman–Weeks method [43]; the temperature of the maximum of the higher temperature endotherm was plotted as a function of the crystallization temperature. The peak temperature was taken for the calculations instead of the onset due to the presence of a low melting endotherm that introduces some error in the determination of the onset of the melting point corresponding to the primary crystallization. Using at least eight experimental points, a linear dependence was observed in the T_c range used in this work. Thus, the extrapolation to $T_c = T_m$ by a linear least squares fit could be performed to calculate T_m^o. For neat PCL, we found a T_m^o of 69.9 ± 1.9 °C, in agreement with values reported in the literature [12,18,44–46]. The melting-point depression exhibited by the PCL fraction with increasing PSMA14 (68.3 ± 2.2 °C and 64.2 ± 1.4 °C for PSMA14/PCL 10/90 and 30/70, respectively) indicates miscibility between PCL and PSMA14 as was previously discussed from the standard DSC scans. Even though the extrapolation implies a significant error, it is frequently used for comparison purposes. Fig. 11 compares the magnitude of the depression found in various PCL blends; it is interesting to note that the PSMA14/PCL system exhibits the highest variations, suggesting a lower Flory–Huggins interaction parameter, χ_{AB}.

From the DSC curves recorded during the isothermal crystallizations, the experimental half-crystallization times, $\tau^{1/2}$, were estimated, and their variation with crystallization temperature is shown in Fig. 12. It is clearly observed that there is a marked dependence on the PSMA14 amount of the supercooling needed for PCL crystallization. For example, when the PSMA14 content reaches 40%, there is an increase at 36 °C of one order of magnitude for the half-crystallization time as compared to neat PCL. This is directly related to the constrains imposed on the crystallizable segments due to the presence of a more rigid polymer, PSMA14, as a consequence of the miscibilization.

In order to gain a preliminary insight of the phase diagram, we thermally treated the blends in the composition range

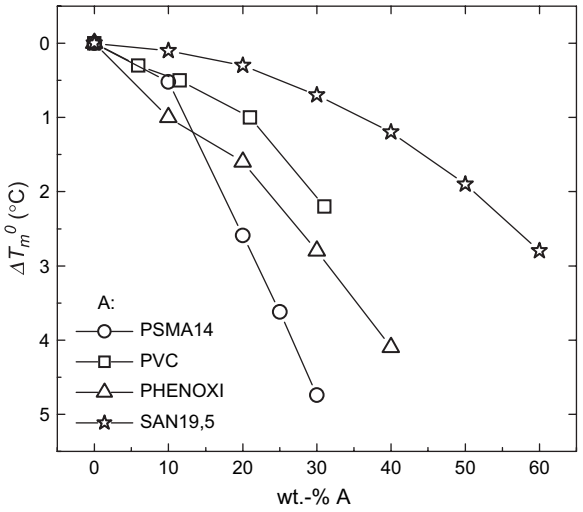

Fig. 11. Equilibrium melting-point depression of the PCL fraction in blends A/PCL as a function of the amorphous polymer A content. (○) This work, (△) [10], (□) [5],(☆) [15].

studied here, at 190 °C for 30, 60 and 180 min under vacuum. Then, the samples were quenched down to −20 °C. The blends with high PSMA14 content did not show variations in their thermal behavior with the annealing time at high temperature. The results for the other compositions are displayed in Table 1.

It can be noted that while the pure PCL does not present significant changes in T_c with the annealing time, blends 30/70 and 10/90 exhibit a progressive increase of the PCL T_c as compared with the untreated sample. This variation is of up to 4.3 °C at 190 °C and 8 °C at 210 °C, i.e. the crystallization temperature tends towards the crystallization temperature of pure PCL. In a previous work [21], it was demonstrated that neither variations of the molecular weight nor chemical reactions between the components occur under these conditions. Therefore, we speculate that the increase of T_c can be attributed to the occurrence of a phase separation process that produces a PCL-rich phase and a PCL-poor phase. In the former

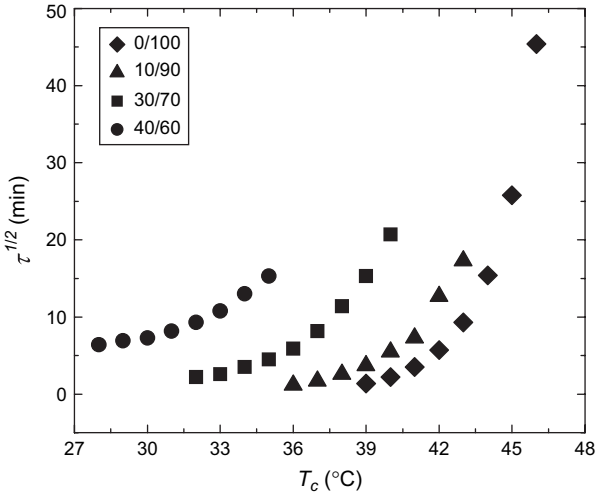

Fig. 12. Experimental half-crystallization times as a function of isothermal crystallization temperature for the indicated PSMA14/PCL compositions.

Table 1
Variation of the PCL crystallization temperature with the thermal treatment

PSMA14/PCL	T_c (wtt)[a] (°C)	T_c (30 min) (°C)	T_c (60 min) (°C)	T_c (180 min) (°C)	T_c (60 min) (°C)	T_c (180 min) (°C)
		190			210	
0/100	30.6	31.5	31.3	30.6	–	–
10/90	26.8	28.8	28.1	30.3	–	–
30/70	16.8	18.1	19.8	21.1	22.4	24.9

[a] wtt: without thermal treatment.

phase, the crystallization of the PCL would be favored with the consequent increase of T_c. These changes occur both by increasing the annealing time or the annealing temperature as shown in Table 1. Additionally, the opposite behavior was found when a PSMA14/PCL 20/80 blend was annealed at 170 °C for times that varied between 3 and 180 min; in that case a decrease of T_c from 23.2 °C down to 17.5 °C was observed. On the basis of the results previously discussed, it can be argued that the PSMA14/PCL system exhibits a phase diagram of the LSCT type. Then, at temperatures up to 170 °C the system has only one phase until it crystallizes, but at a temperature of 190 °C or higher, phase separation takes place and two liquid phases coexist, at least for 30/70 and 10/90 compositions. In order to corroborate this behavior, we treated again the same 30/70 blend sample that had been annealed at 210 °C for 180 min; i.e. we annealed it at 140 °C for 180 min. As a result, the crystallization temperature decreased from 24.9 °C to 22.3 °C. This corroborates the existence of LCST diagram in the sense that at 140 °C, without shear, the initial steps of miscibilization of the previously segregated phases are taking place; i.e. the process is reversible.

4. Conclusions

The combined results of calorimetric, dielectric and morphological studies on PSMA14/PCL blends over the whole composition range allows to draw the following conclusions of the miscibility effect on the blend relaxation dynamics and crystallization kinetics of PCL:

a) Crystallization of PCL in the blend occurs when the PCL content reaches 30% or more. A depression of the PCL melting point and a significant cold crystallization process are detected for the 40/60 blend, showing the intimate mixing of the components with the existence of interactions on a molecular level. This is supported by the interlamellar insertion of the PSMA14, the formation of ring-banded spherulites, and the significant increase in the half-crystallization times.
b) The existence of a miscible interlamellar region leads to a spherulitic extinction ring spacing that becomes larger upon increasing crystallization temperature. Interestingly, it also increases with PSMA14 content. The latter differentiates the PSMA14/PCL system from other PCL blends.
c) Referring to the chain dynamics, our TSDC results indicate that even the short-range reorientations of the PCL dipoles are affected by blending. The addition of the rigid PSMA14 to PCL causes the hindering of the pre-cooperative motions usually assigned to the β relaxation in the presence of PCL crystalline regions.
d) The segmental dynamics represented by the α mode, show the presence of two distinct compositional variations one for each component. On the other hand, the broad enthalpic steps observed by DSC are representative of the glass transition of the blend bulk composition and follows Fox's predictions. The two dynamic glass transitions are attributed to the concentration fluctuations originated by chain connectivity effects. Their compositional variation is very well described by the self-concentration model by assuming that the Kuhn's length is the relevant scale for the cooperative mobility, and that the Fox dependence is preserved when using effective concentrations. It is to be noted that the good quantitative agreement found here excludes the need to consider the effect of thermal concentration fluctuations that have been used in other blend systems. The PSMA/PCL blend system has been shown to follow all the predictions of the Lodge and McLeish model. In the PC/PCL blend system [4], which is almost athermal, i.e. $\chi_{AB} \sim -0.09$ [44,47], the use of Brekner equation was needed to describe the composition dependences of the bulk and effective T_gs. For the PSMA/PCL blend system under study, where the presence of molecular interactions has been suggested, the Fox equation predicts precisely our experimental results for the bulk T_gs. Therefore, a good fit to the Fox equation cannot be the sole criterion to suggest athermal mixing.

Acknowledgements

We are indebted to FONACIT (Project G97000594) for partial funding of this research. D.N. acknowledges her Research Assistanceship from Universidad Simón Bolívar.

References

[1] Paul DR, Bucknall CB. Formulation. In: Polymer blends, vol. 1. USA: John Wiley & Sons; 2000.
[2] Katana G, Fischer EW, Hack TH, Abetz V, Kremer F. Macromolecules 1995;28:2714.
[3] Chung GC, Kornfield JA, Smith SD. Macromolecules 1994;27:964.
[4] Herrera D, Zamora JC, Bello A, Grimau M, Laredo E, Müller AJ, et al. Macromolecules 2005;38:5109.
[5] Eastmond GC. Adv Polym Sci 2000;49:59.
[6] Phud'homme RE. Polym Eng Sci 1982;22:90.
[7] Ong CJ, Price FP. J Polym Sci Polym Symp 1978;63:45.

[8] Chen HL, Li LJ, Lin TS. Macromolecules 1998;31:2255.
[9] Defiew G, Groeninckx G, Reynaers H. Polymer 1989;30:595.
[10] Defieuw G, Groeninckx G, Reynaers H. Polymer 1989;30:2164.
[11] Wang J, Cheung MK, Mi Y. Polymer 2002;43:1357.
[12] Balsamo V, Calzadilla N, Mora G, Müller AJ. J Polym Sci Part B Polym Phys 2001;39:771.
[13] Hernández MC, Laredo E, Bello A, Carrizales P, Marcano M, Balsamo V, et al. Macromolecules 2002;35:7301.
[14] Ikehara T. Polymer 2000;41:7855.
[15] Kressler J, Kammer HW. Polym Bull 1988;19:283.
[16] Kressler J, Svoboda P, Inoue T. Polymer 1993;34:3225.
[17] Kummerlowe C, Kammer HW. Polymer Networks Blends 1995;5:132.
[18] Wang Z, Jiang B. Macromolecules 1997;30:6223.
[19] Defiew G, Groeninckx G, Reynaers H. Polymer 1989;30:2158.
[20] Vanneste M, Groeninckx G. Polymer 1997;38:4407.
[21] Balsamo V, Gouveia L, Herrera L, Laredo E, Méndez B. Revista Latinoamericana de Materiales y Metalurgia 2004;24:17.
[22] Zetsche A, Fischer EW. Acta Polym 1994;45:168.
[23] Lodge TP, McLeish TCB. Macromolecules 2000;33:5278.
[24] Bittiger H, Marchessault RH, Niegisch WD. Acta Crystallogr Sect B 1970;26:1923.
[25] Laredo E, Grimau M, Müller A, Bello A, Suarez N. J Polym Sci Part B Polym Phys 1996;34:2863.
[26] Kammer HW, Kummerlowe C. In: Advances in polymer blends and alloys technology, vol. 5. London: CRC-Taylor & Francis; 1994. p. 132.
[27] Chiu SC, Smith TG. J Appl Polym Sci 1984;29:1797.
[28] Vanneste M, Groeninckx G. Polymer 1994;35:1051.
[29] Li W, Yan R, Jian B. Polymer 1992;33:889.
[30] Wang Z, Lijia AN, Jiang B, Wang X, Zhao H. Polym J 1998;30:206.
[31] Balsamo V, von Gyldenfeldt F, Stadler R. Macromol Chem Phys 1996;197:3317.
[32] Albuerne J, Márquez L, Müller AJ, Raquez JM, Degee Ph, Dubois Ph, et al. Macromolecules 2003;36:1633.
[33] Nojima S, Wang DJ, Ashida T. Polym J 1991;23:1473.
[34] Lotz B, Cheng SZD. Polymer 2005;46:577.
[35] Morin D, Zhao Y, Prud'homme RE. J Appl Polym Sci 2001;81:1683.
[36] Wang Z, Wang X, Yu D, Jiang B. Polymer 1997;38:5897.
[37] Schulze K, Kressler J, Kammer HW. Polymer 1993;34:3704.
[38] Briber RM, Khoury F. Polymer 1987;28:38.
[39] Briber RM, Khoury F. J Polym Sci B Polym Phys 1993;31:1251.
[40] Grimau M, Laredo E, Perez Y, Bello A. J Chem Phys 2001;114:6417.
[41] Leroy E, Alegria A, Colmenero J. Macromolecules 2002;35:5587.
[42] Fetters LJ, Lohse DJ, Richter D, Witten TA, Zirkel A. Macromolecules 1994;27:4639.
[43] Wünderlich B. Crystal melting. In: Macromolecular physics, vol. 3. New York: Academic Press; 1980. p. 33–36.
[44] Jonza JM, Porter RS. Macromolecules 1986;19:1946.
[45] Phillips PJ, Rensch GJ, Taylor KD. J Polym Sci Part B Polym Phys 1987;25:1725.
[46] Neo MK, Goh SH. Eur Polym J 1991;27:927.
[47] Hatzius K, Li Y, Werner M, Jungnickel BJ. Angew Makromol Chem 1996;243:177.